XIV International Conference on Computational Plasticity. Fundamentals and Applications
COMPLAS XIV
E. Oñate, D.R.J. Owen, D. Peric & M. Chiumenti (Eds)

UNCOUPLED MATERIAL MODEL OF DUCTILE FRACTURE WITH DIRECTIONAL PLASTICITY

MIROSLAV ŠPANIEL*, TOMÁŠ MAREŠ*, JIŘÍ KUŽELKA*, FRANTIŠEK ŠEBEK † AND JAN DŽUGAN°

*Czech Technical University in Prague (CTU)
Faculty of Mechanical Engineering
Technická 4, 166 07, Prague, Czech Republic
e-mail: miroslav.spaniel@fs.cvut.cz, web page: http://www.ctu.cz

†Brno University of Technology
Faculty of Mechanical Engineering
Technická 2896/2, 616 69 Brno
e-mail: sebek@fme.vutbr.cz - Web page: http://www.fme.vutbr.cz

°Comtes FHT a.s.
Faculty of Mechanical Engineering
Prøumyslová 995, Dobřany 334 41, Czech Republic
e-mail: jdzugan@comtesfht.cz - Web page: http://www.comtesfht.com

Key words: directional distortional hardening, ductile fracture

Abstract. Proposed paper deals with the application of plastic response with directional distortional hardening (DDH) in uncoupled ductile fracture model and comparison of the results with the same ductile fracture model based on isotropic J2 plasticity. The results of simulations have proven not negligible role of model of plasticity and the response of the model with DDH plasticity is closer to reality then the one of the model with isotropic plasticity.

1 INTRODUCTION

Ductile fracture plays not negligible role in industry. For example safety evaluation of vehicles in case of crash, design and optimization of forming processes, limit analysis of steel structures, etc. may be based on computational models of ductile fracture. Ductile fracture is understood as an integrity loss of bodies due to process of material damaging with significant dissipation of strain energy in conditions of monotonic loading. In finite element calculations ductile fracture is usually performed using constitutive models based on progressive damage following plastic straining. Phenomenological material models describing ductile damage in continuum mechanics mostly act as extension of plastic response models. However damage can be represented as directional, scalar damage parameter is introduced in most application. Damage increment is based on plastic strain

increment. Plastic strain increment is usually scaled such a way, that at point of plastic instability (necking) the integral value of damage reaches unity. The dependence of scale factor on actual stress and/or strain state introduces the dependence of damage on loading path. From the point of view of interpretation of real process inside material the ductile damage material models anticipate the damage to occur on the basis of two different mechanisms: 1) Initiation, growing and connecting of micro–cavities that dominates in domains with tri-axial tensional stress. Load carrying cross section is reduced during damage process and finally leads to failure. Based on representative volume with cavity some micro mechanical continuum models were derived (Rice and Tracey, 1969, etc), that proved exactly the dominant role of stress triaxiality for this damage mechanism occurrence. Stress triaxiality is dimensionless parameter based on stress components that expresses contribution of hydrostatic tension in actual stress state. However models based purely on this damage concept exhibit unrealistic response in domains at which pressure and/or shear stress are dominant. 2) Occurence of localized shear strain in plane of maximal shear stress that holds an angle 45° with first principal plane. Lode angle is another dimensionless stress component parameter, that expresses contribution of shear stress in actual stress state. Based on the interconnection between constitutive models of plastic response and constitutive models of ductile damage two basic categories of ductile damage constitutive models can be distinguished: Uncoupled ductile damage models and coupled ductile damage models. Uncoupled models, simply said, separate plastic response and ductile damage. Parameters of plasticity are not influenced by damage. Coupled models modify plastic response in dependence on damage. Coupled models are generally more complex and they are expected to be closer to reality. On the other hand their complexity causes significant calibration costs in comparison to uncoupled models. Easier calibration process is an essential advantage of uncoupled material models. The calibration of plastic response and calibration of ductile damage can be separated. The calibration is distinctly easier if the uncoupled material model is used.

Most used constitutive models of plastic response of metallic materials in engineering computational mechanics are based on Von Mises plastic condition with either isotropic, either kinematic hardening and associative plastic flow rule. In our previous work we have found uncoupled models based on Von Mises plasticity with isotropic hardening acceptable, except for the response of parts with higher stress concentration [1].

This paper deals with the application of model of plastic response with directional distortional hardening (DDH), that allows to control both position and shape of plastic surface in ductile fracture model described above and comparison of the results with the same ductile fracture model based on Von Mises plasticity with isotropic hardening. Calibration experiments using both smooth and notched round bars, small-punch test, and NT tension-torsion specimens made of steel 08CH18N10T had been performed in the past and referred in [1].

2 DUCTILE DAMAGE MODEL

Material models discussed in this paper are based on incremental model of plastic response with Von Mises condition of plasticity and isotropic hardening (further VMI) or

on incremental model of plastic response with directional distortional hardening (further DDH), and phenomenological model of ductile damage according to Bai–Wierzbicki.

2.1 Plastic response models

Both plastic response models DDH and VMI are based on yield condition and flow rule. Yield condition of DDH, resp. VMI is expressed as

$$f_{DDH} = (\mathbf{S} - \alpha) : \mathbf{H} : (\mathbf{S} - \alpha) - k^2 = 0\,, \quad \text{resp.} \quad f_{VMI} = \mathbf{S} : \mathbf{S} - k^2 = 0\,\cdot \tag{1}$$

The deviatoric part $\mathbf{S}$

$$\mathbf{S} = \sigma + p\mathbf{I} \tag{2}$$

of stress tensor, σ is used in yield conditions as the independence of plastic flow onset on hydrostatic pressure is generally accepted for metallic material. Hydrostatic stress, p, is defined by

$$p = -\frac{1}{3}\mathrm{tr}\,(\sigma)\,\cdot \tag{3}$$

Geometric interpretation of yield condition is usually provided in the space of principal deviatoric stresses (three–dimensional space at which the point $[S_1, S_2, S_3]$ represents the deviatoric stress principal components S_1, S_2, and S_3). It is in evidence, that VMI yield condition represents the surface of sphere with center at origin of principal deviatoric stress space and radius of k. DDH yield condition employs the deviatoric back–stress α determining the location of yield surface, k determines the size of yield surface. Fourth order tensor $\mathbf{H}$ represents the distortion of yield surface. Let's note, that if $\mathbf{H}$ equal unity, DDH becomes Von Mises with kinematic hardening. Associative flow rule in form

$$\dot{\varepsilon}^p = \lambda \frac{\partial f}{\partial \sigma} \tag{4}$$

has been adopted in both DDH and VMI models. Detailed description of VMI plastic response model is well known. In this work native implementation provided within Simulia/Abaqus FE code has been used. Theoretical description of DDH can be found in [3]. The implementation according to [2] in form of so called "alpha model" has been provided by our colleagues as user subroutine under Simulia/Abaqus FE code.

2.2 Ductile damage model

Ductile damage model in this work follows the damage mechanics concept with cumulative scalar damage parameter

$$\omega = \int_0^t \frac{\dot{\bar{\varepsilon}}_{pl}\mathrm{d}t}{\bar{\varepsilon}_f\,(\eta,\ \xi)}\,. \tag{5}$$

Plastic strain intensity rate, $\dot{\bar{\varepsilon}}_{pl}$, is defined as

$$\dot{\bar{\varepsilon}}_{pl} = \sqrt{\frac{2}{3}\dot{\varepsilon}_{pl} : \dot{\varepsilon}_{pl}}\,. \tag{6}$$

Fracture locus $\bar{\varepsilon}_f(\eta,\ \xi)$ expresses the dependence of equivalent plastic strain at the instant of onset of fracture on stress state represented by dimensionless parameters–stress triaxiality, η, resp. Lode parameter, ξ. These parameters are defined using second, J_2, resp. third, J_3, invariant of deviatoric stress

$$J_2 = \frac{1}{2}\mathbf{S} : \mathbf{S} = \frac{1}{2}\left(S_1^2 + S_2^2 + S_3^2\right)\,, \quad \text{resp. } J_3 = \det\mathbf{S} = S_1 S_2 S_3\,, \tag{7}$$

and, Von Mises stress, q,

$$q = \sqrt{3J_2}\,. \tag{8}$$

Then stress triaxiality, resp. Lode parameter is defined as

$$\eta = -\frac{p}{q}\,, \quad \text{resp.} \quad \xi = \frac{27}{2}\frac{J_3}{q^3}\,. \tag{9}$$

If we kept constant both stress triaxiality, η_0, and Lode parameter, ξ_0, during whole loading, then fracture occured at instant t_{crit}, when accumulated equivalent plastic strain, $\bar{\varepsilon}_{pl}$ equal $\bar{\varepsilon}_{f0} = \bar{\varepsilon}_f(\eta_0,\ \xi_0)$

$$\bar{\varepsilon}_{pl} = \int_0^{t_{crit}} \dot{\bar{\varepsilon}}_{pl}\mathrm{d}t = \bar{\varepsilon}_f(\eta_0,\ \xi_0)\,, \tag{10}$$

and critical damage, ω_{crit}, at fracture onset has to be, according to (5)

$$\omega_{crit} = \frac{1}{\bar{\varepsilon}_f(\eta_0,\ \xi_0)}\int_0^{t_{crit}} \dot{\bar{\varepsilon}}_{pl}\mathrm{d}t = 1\,. \tag{11}$$

Assuming the damage to be proportional, we utilize (5) to express the damage caused by plastic straining during the loading history from beginning up to time t with both stress triaxiality and Lode parameter varying. Fracture onset occurs when damage reaches critical value

$$\omega = \omega_{crit} = 1\,. \tag{12}$$

Fracture locus suggested by Bai and Wierzbicki in [4] has form

$$\begin{aligned} \bar{\varepsilon}_f(\eta,\xi) &= \left[\frac{1}{2}\left(D_1 e^{-D_2\eta} + D_5 e^{-D_6\eta}\right) - D_3 e^{-D_4\eta}\right]\xi^2 + \\ &+ \frac{1}{2}\left(D_1 e^{-D_2\eta} - D_5 e^{-D_6\eta}\right)\xi + D_3 e^{-D_4\eta}. \end{aligned} \tag{13}$$

Material parameters D_1, D_2, D_3, D_4, D_5, and D_6 have to be determined on the base of experiments. This ductile damage model has been used to extend both VMI and

DDH plastic response model. These extensions are further referred as VMI based Bai–Wierzbicki ductile fracture model (VMIBW), resp. DDH based Bai–Wierzbicki ductile fracture model (DDHBW).

Artificial degradation on the base of Hillerborg's fracture energy is implemented in both VMIBW and DDHBW in order to guarantee sufficient smoothness of fracture process simulation. Instead of immediate removing the stress gradual loss of material stiffness in term of Young modulus, E, driven by parameter of degradation $D \in \langle 0; 1 \rangle$, is employed in material point of FE model since damage reached it's critical value

$$E^* = (1 - D)\, E \cdot \tag{14}$$

3 CALIBRATION

As both VMIBW and DDHBW are uncoupled ductile damage models, the plastic response has been calibrated separately using the same test performed on smooth round bar. Further the calibration of fracture locus will be discussed. Tensile experiments with both smooth and notched round bars using four different notch radii, tension-torsion experiments using NT specimen with five different proportional loading paths, and small punch test have been utilized to calibrate fracture loci for both VMIBW and DDHBW models. Calibration experiments are briefly listed in table 3. Each row in the table

Table 1: Complete portfolio of experiments, that have been used to calibrate both VMIBW and DDHBW.

Smooth, resp. notched round bars, tension					
Label	R [mm]	d [mm]	N	ΔL_f [mm]	Remark
R_0	∞	12	5	14	Smooth bar
R_{15}	15	12	2	8.1	Notched bar
R_7	7	12	2	6.6	Notched bar
R_4	4	12	5	5.7	Notched bar
NT specimens, proportional tension–torsion					
Label	p [mm]	cal. quantity	N	$\Delta L_f or \Delta\varphi_f$ [mm], or [1]	Remark
NT_3	0.000000000	$\Delta\varphi$	2	0.6637	Pure torsion
NT_4	0.000152425	$\Delta\varphi$	2	0.6744	Tension–torsion
NT_5	0.000304851	$\Delta\varphi$	2	0.5681	Tension–torsion
NT_6	0.001278454	ΔL	2	0.8181	Tension–torsion
NT_7	∞	ΔL	2	0.6027	Pure tension
Small punch test					
Label	D_{punch} [mm]	t [mm]	N	Δu_f [mm]	Remark
SP	2.5	0.5	5	2.05	

represents single calibration case. N for all cases means the number of specimens that had been tested within the case. For smooth/notched round bars R means the radius of the notch, d is the diameter of bar cross-section at notch tip. For NT specimens p describes the loading path as the ratio between the extension ΔL and torsion $\Delta\varphi$

$$p = \frac{\Delta L}{\Delta \varphi} \cdot \tag{15}$$

Proportional loading had been performed, so p is kept constant during loading. For small punch test D_{punch} is the diameter of spherical punch, t is thickness of the penny–like specimen. The calibration is based on critical extensions, critical torsions, or critical

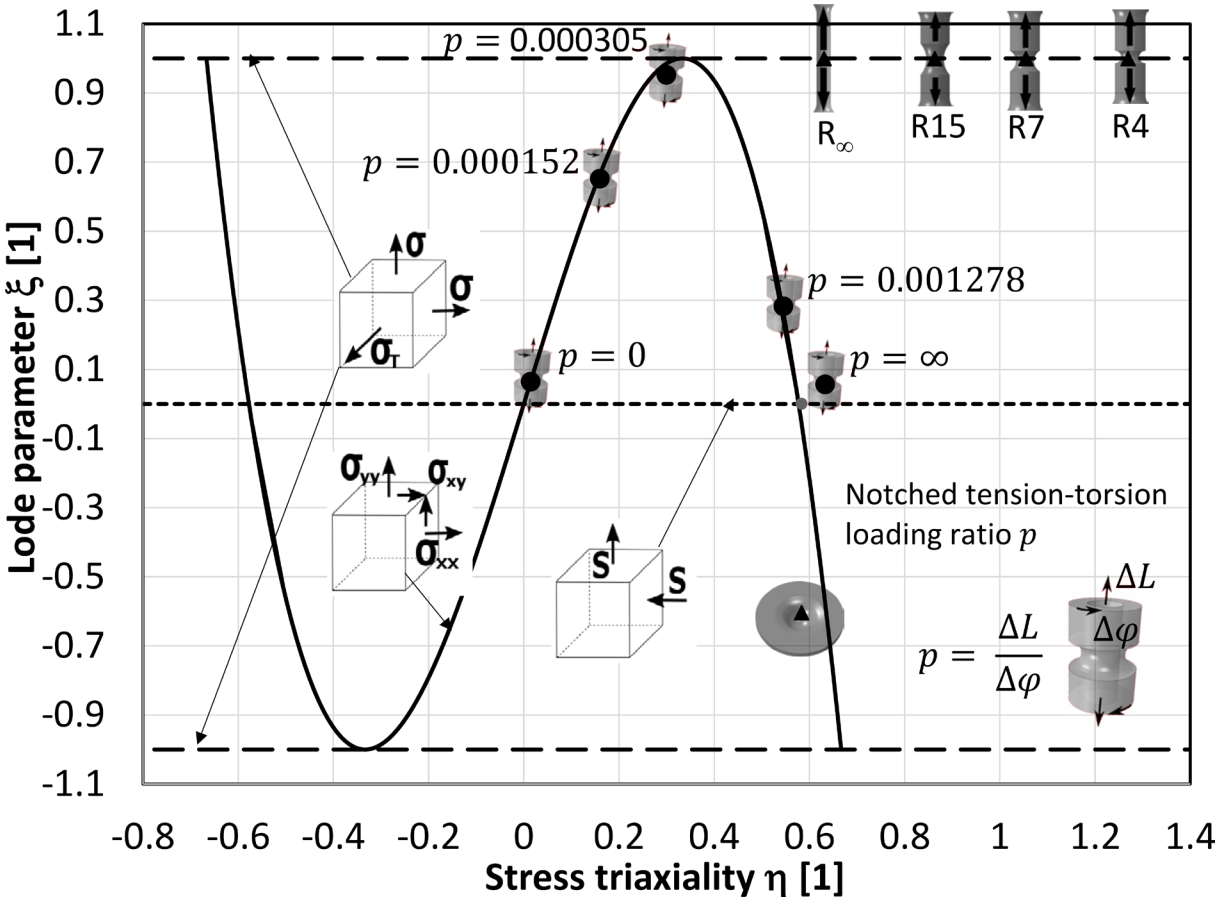

Figure 1: Portfolio of calibration cases.

displacements. For smooth/notched round bars the extension has been measured using extensometer (the fracture of all valid specimens has to occure within the base of extensometer). Critical extension ΔL_f has been determined as average value of extension at fracture onset of all valid specimens. For NT specimens both the extension and the relative torsion has been measured for each specimen. The calibration quantity has been chosen as ΔL or as $\Delta\varphi$ with respect to dominating deformation. Then corresponding critical value ΔL_f or $\Delta\varphi_f$ has been determined as average value of calibration quantity at

fracture onset of all valid specimens as well. For small punch test the punch displacement Δu has been measured. Critical displacement Δu_f has been determined as average value of punch displacements at fracture onset of all valid specimens. Corresponding tensile forces and/or torques have been measured at the same time, so the experimental loading curves can be used to evaluate results of calibration.

Calibration of fracture locus means to determine parameters D_1, D_2, D_3, D_4, D_5, and D_6 of fracture locus (13) providing good approximation of fracture of single specimens. This is usually performed as minimization of target function representing the deviation of FE calculation results and corresponding experiments in average sense over all calibration cases. In this work target function F_ω defined in sense of deviations between critical damage ω_i estimation and it's exact value $\omega_{crit} = 1$ for i^{th} calibration case, averaged over all calibration cases

$$F_\omega = \sqrt[m]{\frac{1}{N}\sum_{i=1}^{N} |1 - \omega_i|^m} \,. \tag{16}$$

ω_i estimation is evaluated by integration up to critical extension, resp. critical torsion, resp. critical displacement

$$\omega_i = \int_0^{\Delta\mathcal{L}_{\mathrm{f,i}}} \frac{\mathrm{d}\bar{\varepsilon}_{pl}}{\bar{\varepsilon}_f\left(\eta,\, \xi\right)} \,, \tag{17}$$

where $\Delta\mathcal{L}_{\mathrm{f,i}} = \Delta L_{f,i}$, resp. $\Delta\mathcal{L}_{\mathrm{f,i}} = \Delta\varphi_{f,i}$, resp. $\Delta\mathcal{L}_{\mathrm{f,i}} = \Delta u_{f,i}$. Let's denote, that initial values of D_1, D_2, D_3, D_4, D_5, and D_6 for minimization of target F_ω have been determined using more conservative approach based on averaging both stress triaxiality and Lode parameter up to critical extension, resp. critical torsion, resp. critical displacement Weighted average values of stress triaxiality for i^{th} calibration case $\eta_{av,i}$ is calculated according to

$$\eta_{av} = \frac{1}{\bar{\varepsilon}_{f,i}} \int_0^{\bar{\varepsilon}_{f,i}} \eta_i\left(\bar{\varepsilon}_{pl}\right) \mathrm{d}\bar{\varepsilon}_{pl} \,, \tag{18}$$

lode parameter weighted average is expressed as

$$\xi_{av} = \frac{1}{\bar{\varepsilon}_{f,i}} \int_0^{\bar{\varepsilon}_{f,i}} \xi_i\left(\bar{\varepsilon}_{pl}\right) \mathrm{d}\bar{\varepsilon}_{pl} \,. \tag{19}$$

The point $[\eta_{av,i},\, \xi_{av,i},\, \bar{\varepsilon}_{f,i}]$ can be determined by this approach for each individual calibration case. Fracture locus should pass these points, so target function

$$F_{av} = \sqrt[m]{\frac{1}{N}\sum_{i=1}^{N} \left|\bar{\varepsilon}_{f,i} - \bar{\varepsilon}_f\left(\eta_{av,i},\, \bar{\theta}_{av,i}\right)\right|^m} \tag{20}$$

can be used. The main disadvantage of this approach is wide range of stress triaxiality η and Lode parameter ξ for some specimen types resulting in non-negligible error due to the averaging of these quantities. On figure 3 single calibration cases are located at stress triaxiality–Lode angle space in sense of average values.

4 RESULTS AND DISCUSSION

Finite element calculation of both VMI and DDH elastic plastic response of all calibration cases have been done. Axisymmetry, resp. cyclic symmetry has been employed in smooth/notched round bars and small punch test FE models, resp. NT FE models to speed up the analyses. Then calibration of fracture loci have been performed. Calibrated parameters are provided in table 4, fracture loci of both VMIBW and DDHBW are plotted in figure reffig:Flocus Finite elements calculations of both VMIBW and DDHBW

Table 2: Fracture locus parameters for both VMIBW and DDHBW.

model	D_1	D_2	D_3	D_4	D_5	D_6
VMIBW	1.14620935	0.92336854	0.52982388	1.3923699	1.84258408	0.62297372
DDHBW	1.24892547	0.77904199	0.6579249	1.4036429	1.61503802	0.7210034

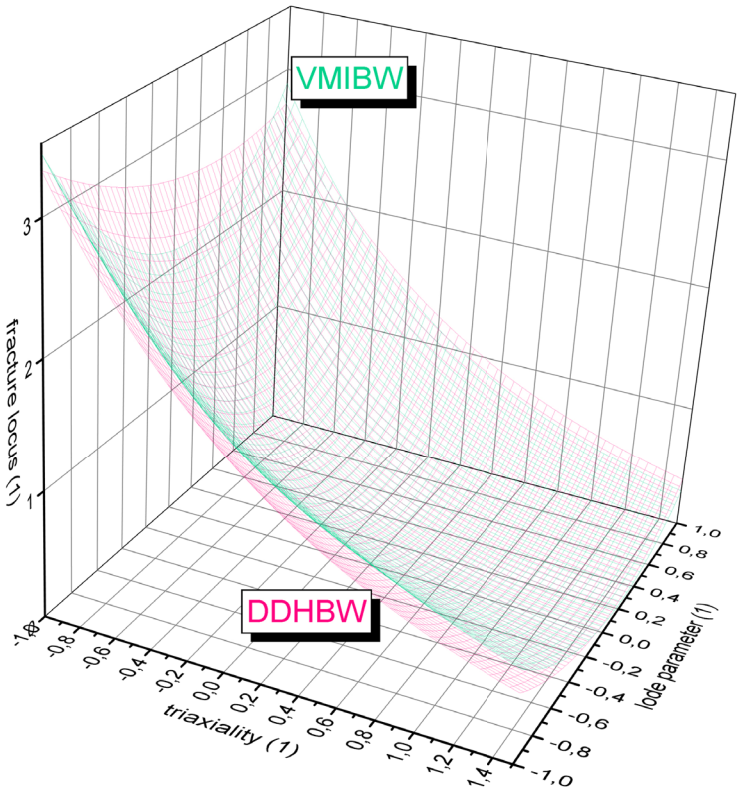

Figure 2: Fracture locus for both VMIBW and DDHBW models

elastic plastic ductile fracture response of selected specimens smooth/notched round bar (including R_1, R_2, that had not been used in calibration) have been done using calibrated fracture loci. The comparison of loading curves $\Delta L - F$ is provided on figures 3, 4, and

5. All these plot show, that DDHBW agreement with experimental data is better than the VMIBW one.

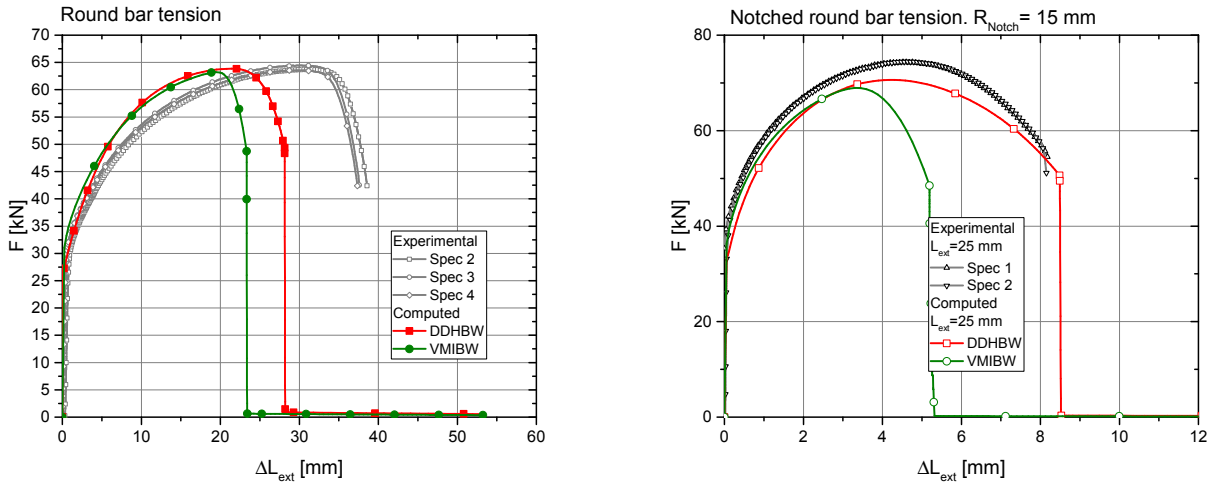

Figure 3: Comparison of experimental loading curves with computed using both VMIBW and DDHBW. Specimens R_0, R_{15}.

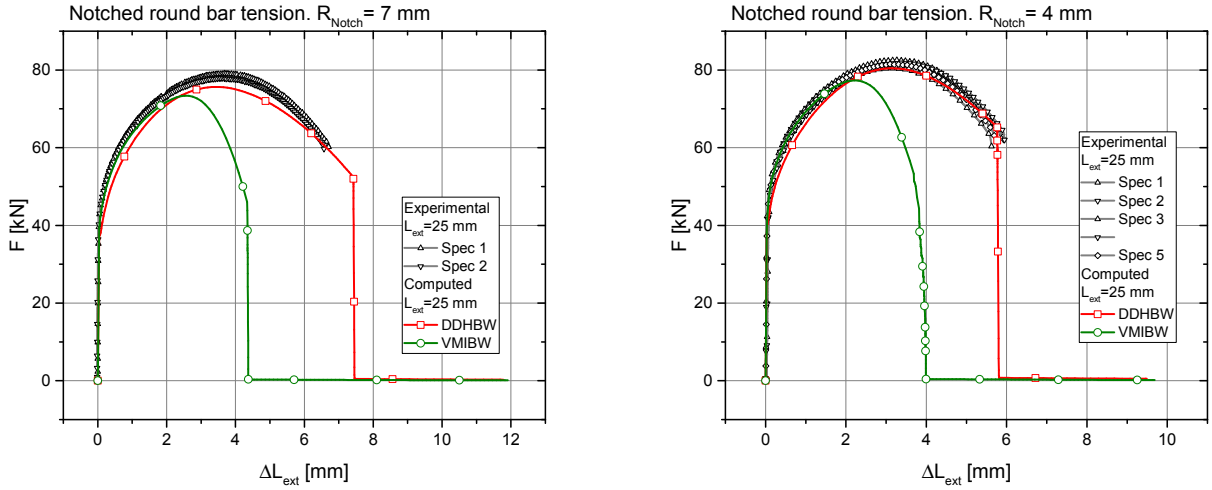

Figure 4: Comparison of experimental loading curves with computed using both VMIBW and DDHBW. Specimens R_7, R_4.

5 CONCLUSIONS

- The results of performed simulations of ductile fracture have proven not negligible role of model of plasticity on the results.
- The results of models with DDHBW elastic plastic ductile fracture model is closer to reality then the results of the model with VMIBW elastic plastic ductile fracture model calibrated with the same portfolio of specimens.

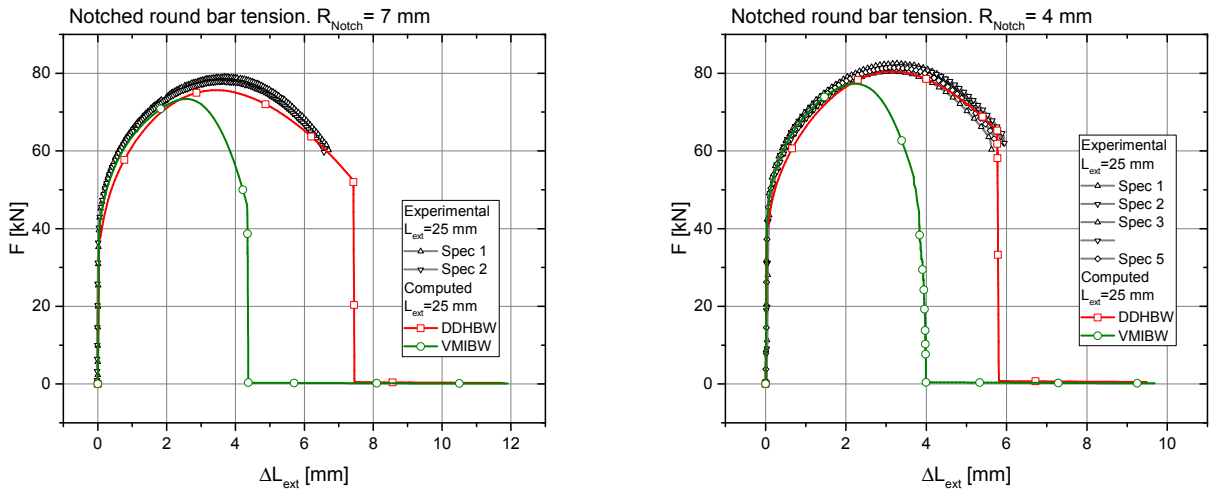

Figure 5: Comparison of experimental loading curves with computed using both VMIBW and DDHBW. Specimens R_2, R_1 had not been used in calibration.

- Using of DDHBW uncoupled ductile fracture model may be an alternative approach to more expensive coupling damage with plasticity if improvement of prediction is needed.

- Further, analyses of more cases, testing of alternative fracture locus formulation with DDH is planed.

6 ACKNOWLEDGMENT

The financial support provided by the Czech Science Foundation (GAČR grant no. 15-20666S) is gratefully acknowledged.

REFERENCES

[1] Španiel, M. Prantl, A. Džugan, J. Røužička, J. and Moravec, M. Calibration of fracture locus in scope of uncoupled elastic-plastic-ductile fracture material models. *Advances in Engineering Software.* (2014) **76**:95-108

[2] Plešek, J. Feigenbaum, H.P. Marek, R. Dafalias, Y.F. Hrubý, Z. and Parma, S. Numerical Implementation of A Model With Directional Distortional Hardening. *Journal of Engineering Mechanics.* (2015) **141, 12**

[3] Feigenbaum, H.P. and Dafalias, Y.F. Directional distortional hardening in metal plasticity within thermodynamics. *International Journal of Solids and Structures.* (2007) **44**:75267542

[4] Bai, Y. and Wierzbicki, T. A new model of metal plasticity and fracture with pressure and lode dependence. *International Journal of Plasticity.* (2008) **24, 6**:10711096